

Supporting Information

Table S1. Characterization of different shaped polymer micelles loaded with DOX.

Sample	Average size (nm)	PDI	Zeta potential(mV)
S ₁	109±2.1	0.126±0.010	-19.8±0.2
R ₁	224±3.2	0.395±0.019	-20.2±0.1
S ₂	136±3.8	0.131±0.023	-23.4±0.2
R ₂	341±5.7	0.412±0.021	-24.1±0.3
S ₁ @DOX	113±1.9	0.119±0.011	-6.4±0.4
R ₁ @DOX	231±2.7	0.412±0.02	-7.2±0.3
S ₂ @DOX	141±3.3	0.129±0.022	-7.9±0.5
R ₂ @DOX	348±6.3	0.432±0.025	-9.1±0.3

Table S2. Characterization of the DOX-loaded different shaped polymer micelles.

Sample	S ₁ @DOX	R ₁ @DOX	S ₂ @DOX	R ₂ @DOX	R ₂ @DOX/Fe ₃ O ₄
LC%(UV-vis)	4.9±0.29	7.0±0.42	5.1±0.96	7.3±0.33	4.3±0.21
EE%(UV-vis)	53.4±2.89	74.7±1.26	54.6±1.43	72.4±3.55	49.6±2.11

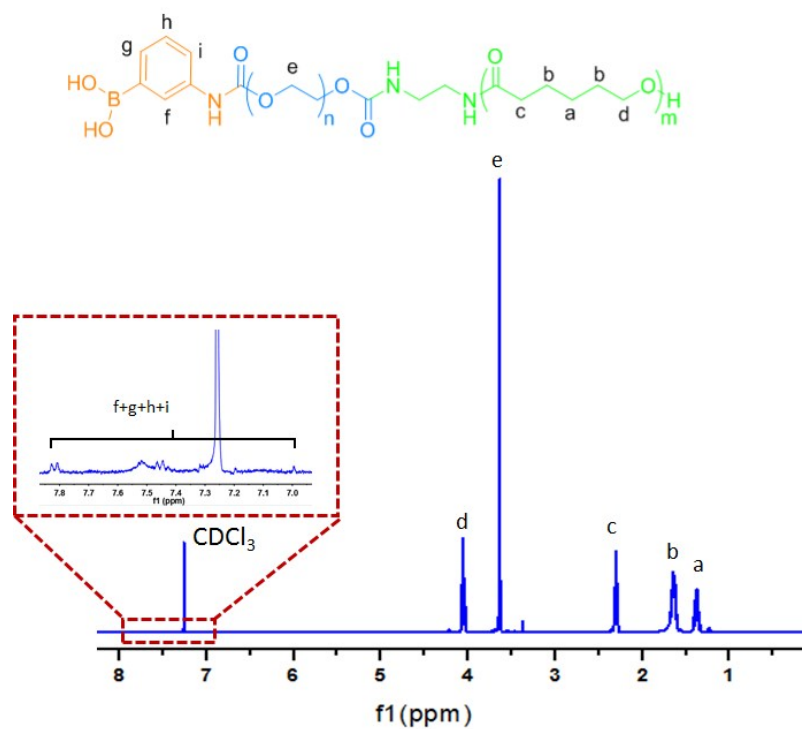


Figure S1. ^1H NMR spectrum of the PBA-PEG-PCL copolymer in CDCl_3 .

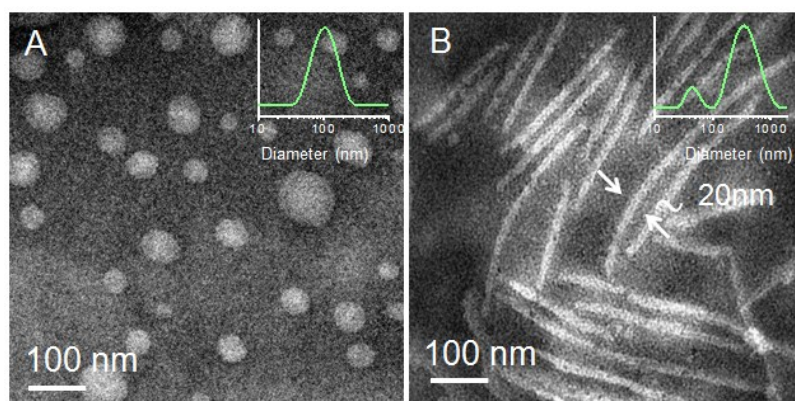


Figure S2. TEM images of micelles with different shapes. (A) mPEG-PCL blank micelles with spherical shape (S_1); (B) mPEG-PCL blank micelles with rod-like shape (R_1). The inserted images are the particle size distribution.

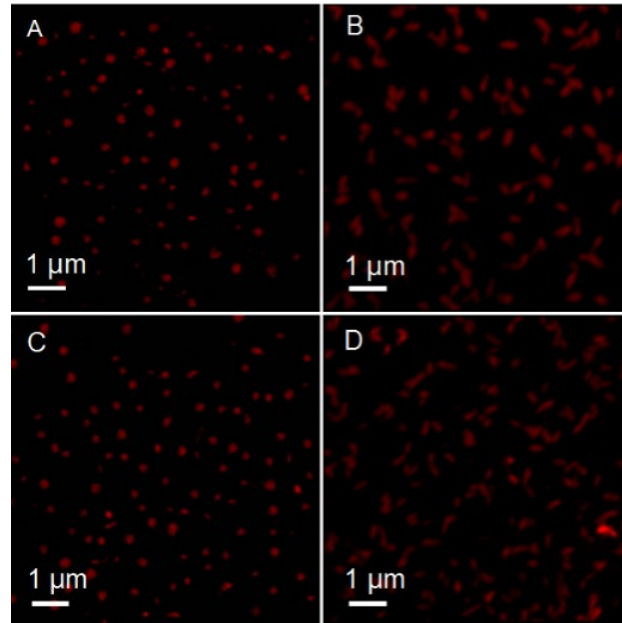


Figure S3. CLSM images of micelles with different drug-loaded morphologies. (A) mPEG-PCL micelles with spherical shape (S_1); (B) mPEG-PCL micelles with rod-like shape (R_1); (C) PBA-PEG-PCL micelles with spherical shape (S_2); (D) PBA-PEG-PCL micelles with rod-like shape (R_2).

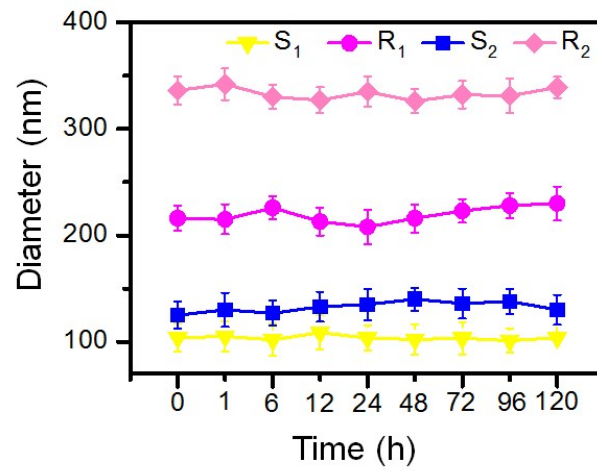


Figure S4. The stability of different shaped micelles at a concentration of 1 mg/mL in 0.9% physiological saline solution over time. S_1 : mPEG-PCL micelles with spherical shape; R_1 : mPEG-PCL micelles with rod-like shape; S_2 : PBA-PEG-PCL micelles with spherical shape; R_2 : PBA-PEG-PCL micelles with rod-like shape.

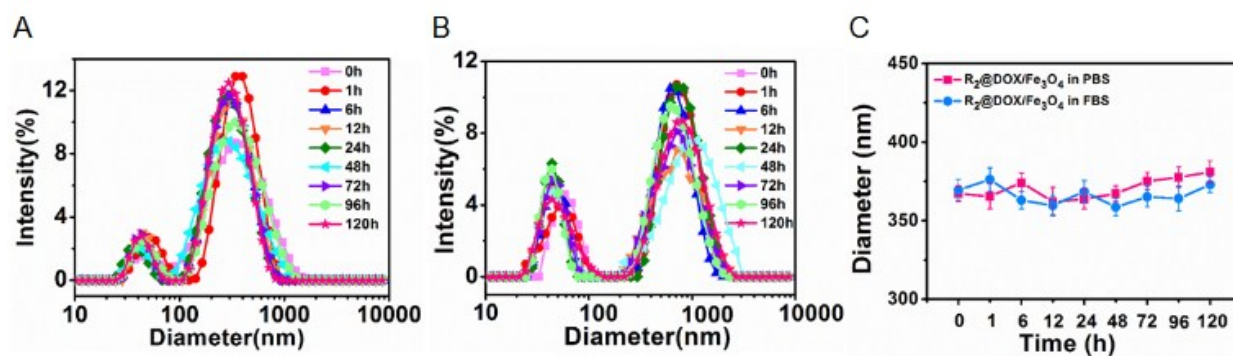


Figure S5. The stability of $R_1@DOX/Fe_3O_4$ micelles at different dispersed media over time. A) $R_1@DOX/Fe_3O_4$ micelles in PBS. B) $R_1@DOX/Fe_3O_4$ micelles in FBS. C) The average size changes of the micelles over time.

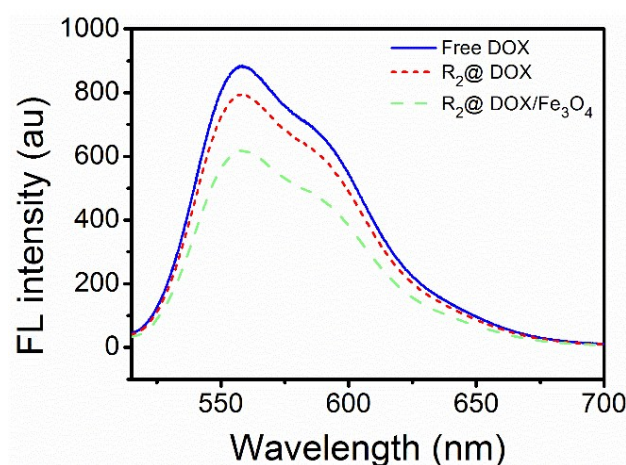


Figure S6. Fluorescence emission spectra of Free DOX, $R_2@DOX$, $R_2@DOX/Fe_3O_4$ (DOX dose is 5 $\mu\text{g/mL}$ in all the three groups).

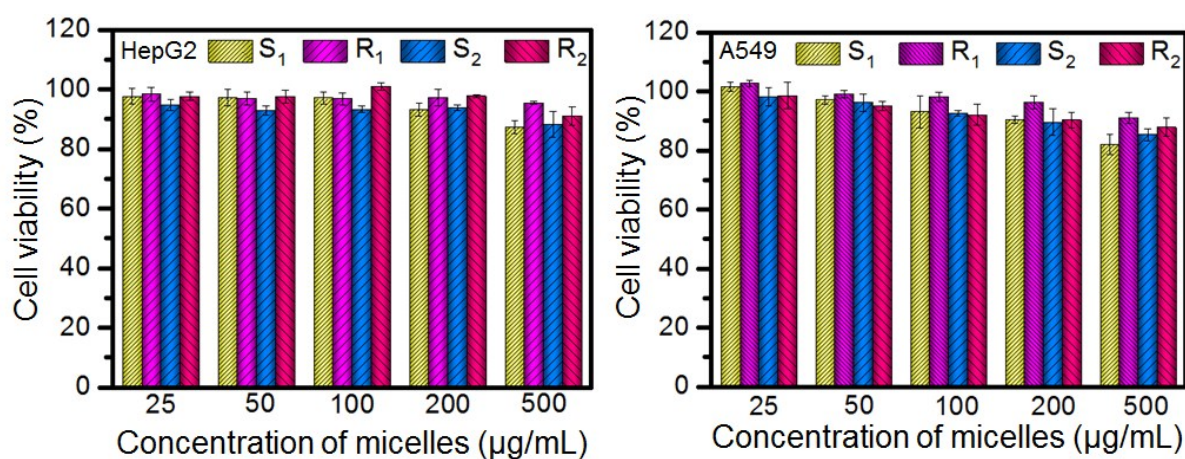


Figure S7. Cell viability of HepG2 cells and A549 cells after incubation with S_1 , R_1 , S_2 and R_2 at different concentrations for 24 h.

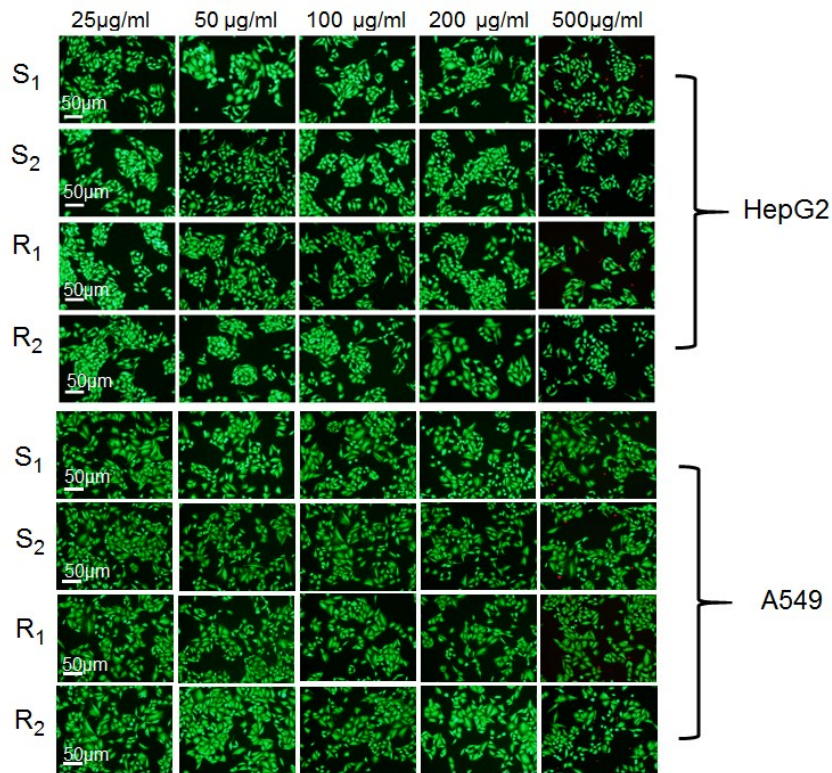


Figure S8. Fluorescence images of HepG2 cells and A549 cells after incubation with S₁, R₁, S₂ and R₂ at different concentrations for 24 h.

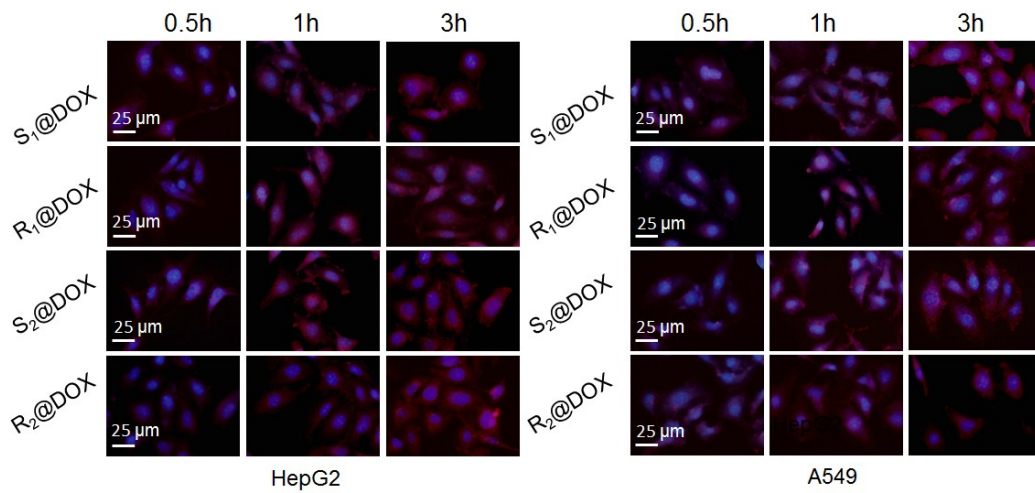


Figure S9. Fluorescence images of cellular uptake of different shaped DOX-loaded micelles after incubation with HepG2 cells and A549 cells for 0.5 h, 1 h and 3 h.

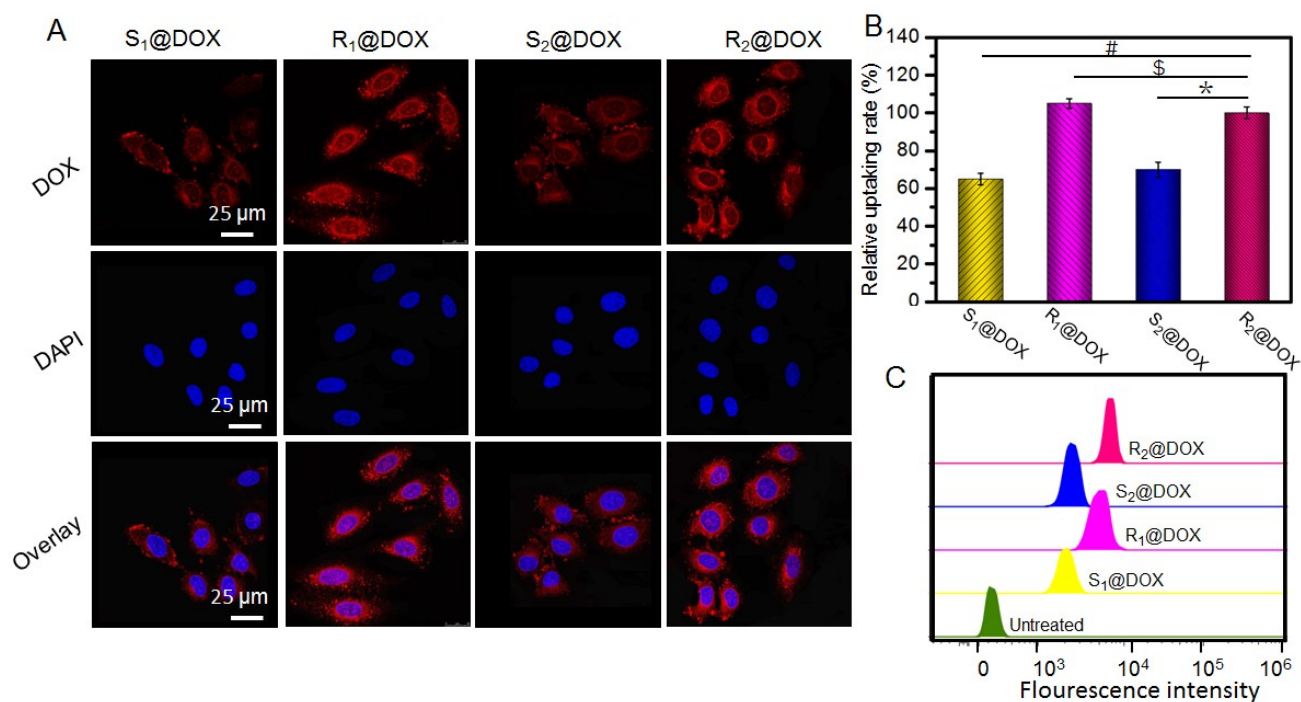


Figure S10. Cellular uptake and intracellular distribution of the DOX-loaded micelles in A549 cells. (A) CLSM image of A549 cells after incubated with S₁@DOX, R₁@DOX, S₂@DOX, R₂@DOX for 3 h. The nuclei were stained with DAPI (blue) and the dose of DOX is 5 μ g/mL. (B) Quantitative analysis of DOX in A549 cells through the Image-Pro Plus 6.0. The S₁@DOX, R₁@DOX and S₂@DOX groups were compared with the R₂@DOX group. The data were shown as the mean \pm standard (SD) (n = 3). \$ (not significant), * (P<0.05), # (P<0.01). (C) Flow cytometry quantitative analysis of HepG2 cells after incubation with free DOX, S₁@DOX, R₁@DOX, S₂@DOX and R₂@DOX for 3 h (DOX dose: 5 μ g/mL).